doi.org/10.1002/cbdv.202300766 Research Article CHEMISTRY & BIODIVERSITY

www.cb.wiley.com

Synthesis and Evaluation of Novel Metacetamol Derivatives with Hydrazone Moiety as Anticancer and Antimicrobial Agents

Sevil Şenkardeş,*[a] İrem Atlıhan,[b] Elif Çayır,[c] Pınar Mega Tiber,[d] Oya Orun,[d] Şeyma Nigiz,[e] Ceren Özkul,[e] Miyase Gözde Gündüz,[f] and Ş. Güniz Küçükgüzel[g]

By exploiting the wide biological potential of the hydrazone scaffold, a series of hydrazone derivatives were synthesized, starting from *N*-(3-hydroxyphenyl)acetamide (metacetamol). The structures of the compounds were determined using IR, ^{1}H and ^{13}C-NMR, and mass spectroscopic methods. The obtained molecules (**3 a**–**j**) were evaluated for their anticancer potential against MDA-MB-231 and MCF-7 breast cancer cell lines. According to the CCK-8 assay, all tested compounds showed moderate to potent anticancer activity. Among them, *N*-(3-(2-(2-(4-nitrobenzylidene)hydrazinyl)-2-oxoethoxy)phenyl)acetamide (**3 e**) was found to be the most effective derivative with an IC_{50} value of 9.89 μM against MDA-MB-231 cell lines. This compound was further tested for its potential effects on the apoptotic pathway. Molecular docking studies was also carried out for **3 e** in the colchicine binding pocket of tubulin. Additionally, compound **3 e** also demonstrated effective antifungal activity, particularly against *Candida krusei* (MIC = 8 μg/ml), indicating that nitro group at the 4th position of the phenyl ring was the most preferable substituent for both cytotoxic and antimicrobial activity. Our preliminary findings suggest that compound **3 e** could be exploited as a leading structure for further anticancer and antifungal drug development.

Introduction

Breast cancer is a significant global health concern and is classified into two major groups based on estrogen receptor (ER) status. ER positive cancers respond to treatment with estrogen or progesterone and are responsible for two-thirds of deaths, while ER negative cancers account for one-third of deaths.[1,2] Effective treatment options for breast cancer, especially ER-negative cancers, are needed to improve patient outcomes.

Cancer patients are more susceptible to microbial infections due to factors such as aggressive therapies, frequent antibiotic use, and compromised immune systems.[3] Neutropenic patients, in particular, are at a higher risk of developing drug-resistant bacterial infections. Candidiasis, a fungal infection, is also a common concern in cancer patients.[4–6]

Hydrazones are a class of organic compounds that contain a hydrazone functional group (–NHN=) and are widely used in various fields including pharmaceuticals, agrochemicals, and materials science.[7] They have shown promising potential in the development of antimicrobial and anticancer drugs. Numerous studies have demonstrated the potent antimicrobial activity of hydrazone-based compounds against various bacterial and fungal pathogens.[8–12] Additionally, hydrazone derivatives have represented promising anticancer activity by inhibiting cancer cell proliferation and inducing apoptosis.[13–19] The mechanism of action of these compounds involves targeting specific cellular pathways and enzymes, facilitated by their multiple hydrogen bond acceptor/donor atoms that can interact with biological targets. Importantly, this functional group is found in several commercially available drugs used to treat diverse diseases including cancer, fungal and bacterial infections (Figure 1).

Due to the crucial role of hydrazone molecules in the pharmaceutical field and the need for targeted chemotherapeutic agents, a series of hydrazones have been developed using metacetamol. Metacetamol, (*N*-(3-hydroxyphenyl)acetamide) is a regioisomer of paracetamol and was chosen in this study, due to the diverse biological activities of its *N*-phenylacetamide moiety, including anticancer and antimicrobial properties.[20–22]

In light of these considerations, we aimed to synthesize new hydrazone derivatives starting from metacetamol (**3 a**–**j**) and to

[a] *S. Şenkardeş*
Marmara University, Faculty of Pharmacy, Department of Pharmaceutical Chemistry, Maltepe, Başıbüyük, 34854 Istanbul, Turkey
E-mail: sevil.aydin@marmara.edu.tr

[b] *İ. Atlıhan*
Marmara University, Institute of Health Sciences, Department of Biophysics, 34865 Istanbul, Turkey

[c] *E. Çayır*
Marmara University, Faculty of Pharmacy, 34854 Istanbul, Turkey

[d] *P. Mega Tiber, O. Orun*
Marmara University, Faculty of Medicine, Department of Biophysics, 34854 Istanbul, Turkey

[e] *Ş. Nigiz, C. Özkul*
Hacettepe University, Faculty of Pharmacy, Department of Pharmaceutical Microbiology, Sıhhiye, 06100 Ankara, Turkey

[f] *M. G. Gündüz*
Hacettepe University, Faculty of Pharmacy, Department of Pharmaceutical Chemistry, Sıhhiye, 06100 Ankara, Turkey

[g] *Ş. G. Küçükgüzel*
Fenerbahçe University, Faculty of Pharmacy, Department of Pharmaceutical Chemistry, Ataşehir, 34758 Istanbul, Turkey

Supporting information for this article is available on the WWW under https://doi.org/10.1002/cbdv.202300766

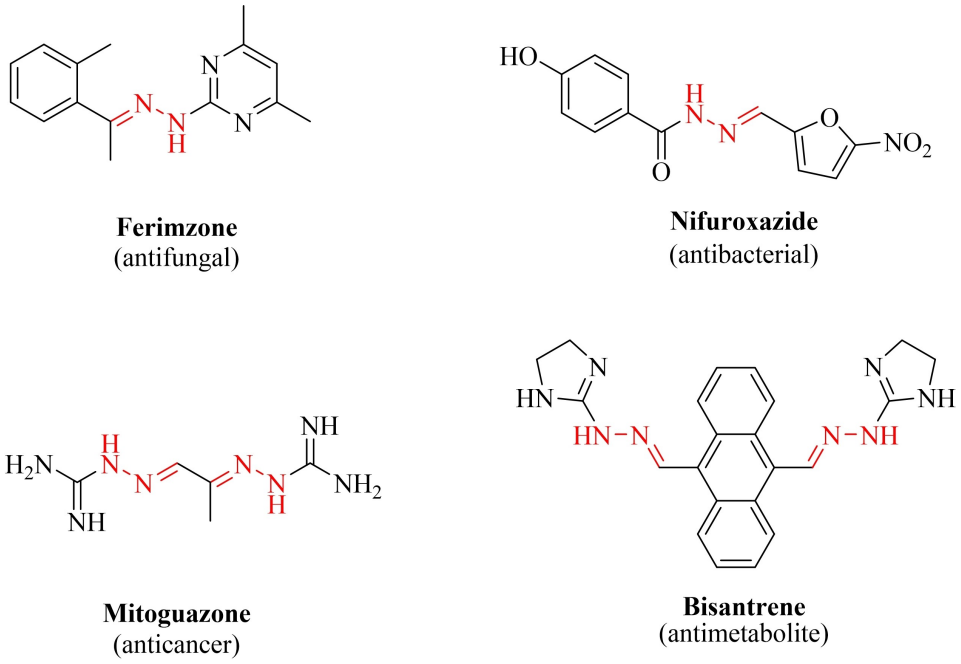

Figure 1. Some commercial drugs derived from hydrazone scaffold.

explore the therapeutic potential of these compounds in treating breast cancer and managing microbial infections commonly observed in cancer patients. For this purpose, the cytotoxic potential of the hydrazone derivatives was assessed against ER-positive (MCF-7) and ER-negative (MDA-MB-231) breast cancer cell lines, and the potential mechanism of cytotoxic activity was investigated. Additionally, the antimicrobial activity of **3a–j** was evaluated against Gram-positive and Gram-negative bacteria, as well as against *Candida* species. This assessment provides insights into the potential of metacetamol-derived hydrazone compounds as dual-function agents that can inhibit tumor growth and offer prophylaxis against microbial infections in cancer patients undergoing chemotherapy treatment.

Results and Discussion

Chemistry

The synthesis of ester **1** and hydrazide **2**, a precursor to the desired new hydrazide-hydrazone derivatives **3a–j**, was carried out following the procedure outlined in Figure 2. Briefly, to prepare hydrazide, *N*-(3-hydroxyphenyl)acetamide (metacetamol) was acquired from Sigma–Aldrich and subjected to refluxing with ethyl bromoacetate under basic conditions to give ethyl 2-(3-acetamidophenoxy)acetate (**1**). Subsequently, the obtained product was treated with hydrazine hydrate in ethanol to yield *N*-(3-(2-hydrazinyl-2-oxoethoxy)phenyl)acetamide (**2**).[23,24] Under reflux conditions for 3–4 h, in the presence of a catalytic amount of glacial acetic acid in ethanol, the condensation reaction of compound **2** with aromatic aldehydes produced hydrazide-hydrazones **3a–j** (Figure 2).

The structures of all the synthesized compounds were characterized using FT-IR, ^{1}H-NMR, ^{13}C-NMR, MS spectroscopy, and elemental analysis, as given in the experimental section. The presence of C=O and C=N stretching vibrations in the range of 1649–1674 cm^{-1} and 1585–1608 cm^{-1}, respectively, confirmed the presence of the acyl hydrazone backbone in all compounds. The ^{1}H and ^{13}C-NMR spectra of the hydrazide-hydrazone compounds showed duplicated signals, indicating the presence of a mixture of syn/anti conformers around the amide bond, not *E/Z* stereoisomers of the imine double bond (Figure 3). Previous literature has demonstrated that the most stable isomer is the *E* geometric isomer, which has been confirmed to be present in DMSO-d_6 solution through various experiments including NOE, NOESY, X-ray diffraction crystallography and conformation analysis.[25–27] The ^{1}H-NMR spectra of compounds **3a–j** displayed two sets of singlet signals at 4.59–4.67/5.03–5.17 and 7.95–8.33/8.18–8.69 ppm corresponding to the OCH_2 and N=CH protons, respectively. Similarly, separated singlet signals between 11.47–11.87 ppm were observed, corresponding to the C(O)NH protons. The acetamide protons appeared between 9.91–9.97 ppm as two separate singlet signals.

The ^{13}C-NMR spectra of compounds **3a–j** synthesized also demonstrated duplicated signals, suggesting the presence of a mixture of conformational stereoisomers.[25] Two signals were observed for the carbonyl carbon (**C**=O), with peaks assigned to the antiperiplanar and synperiplanar conformers. The methylene ($\mathbf{C}H_2$) and azomethine (**C**=N) carbons also yielded two signals.

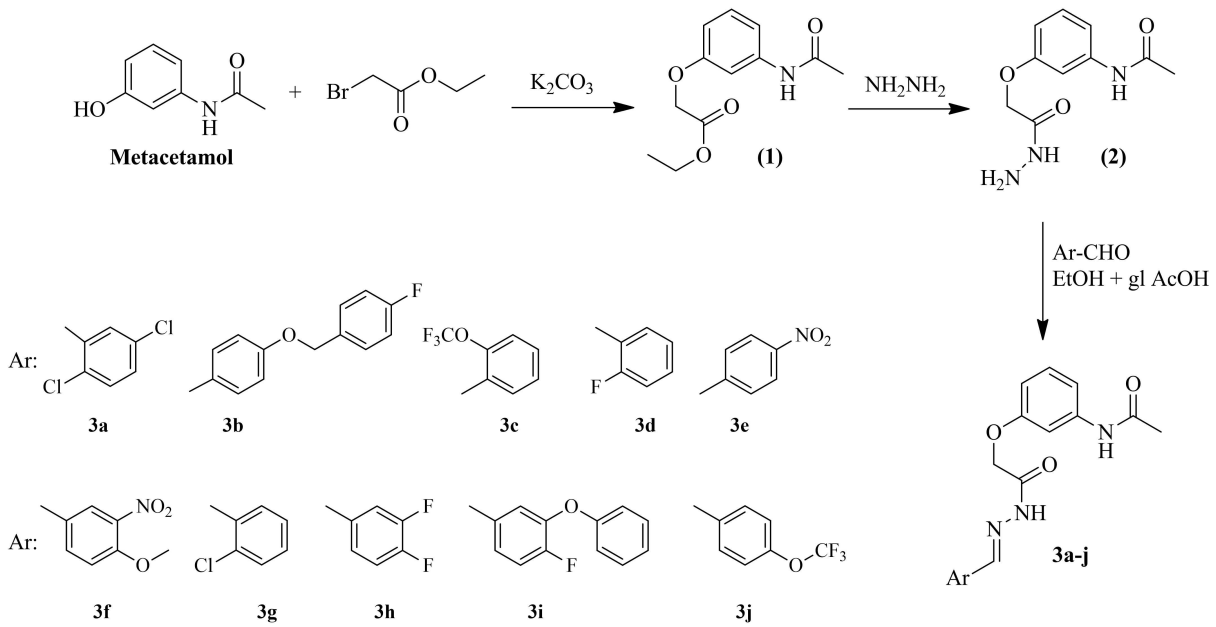

Figure 2. Synthetic route for the preparation of compounds **3a–j**.

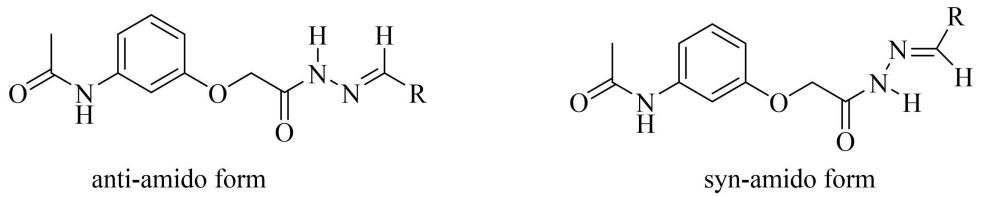

Figure 3. Representation of amido forms of compounds **3a–j**.

Biological evaluation

Antimicrobial activity

The compounds **3a–j** were screened for their antibacterial activity against a panel of reference bacterial strains including *Staphylococcus aureus* ATCC 29213, *Enterococcus faecalis* ATCC 29212, *Escherichia coli* ATCC 25922, and *Pseudomonas aeruginosa* ATCC 27853 using ciprofloxacin as reference drug. Furthermore, **3a–j** were also tested for antifungal activity against yeast strains *Candida albicans* ATCC 90028, *Candida parapsilosis* ATCC 90018, and *Candida krusei* ATCC 6258 employing fluconazole as the standard. The results of the antimicrobial activity screening of the tested compounds are summarized in Table 1.

Based on the obtained data, the compounds exhibited MIC values ranging from 64 μg/mL to 1024 μg/mL against bacteria. Notably, compounds **3a**, **3c**, **3f** and **3g** demonstrated moderate antibacterial activity against *E. faecalis* with a MIC value of 64 μg/mL. Furthermore, in the antifungal screening, several derivatives displayed a broad spectrum of activity against the tested fungi. Among them, compound **3e**, which is 4-nitrophenyl derivative, exhibited superior activity against *C. krusei* compared to the reference drug fluconazole, with a MIC of 8 μg/mL (Table 1). It is important to highlight the significance of this finding as *C. krusei* is a common causative agent of invasive candidiasis and non-albicans candidemia worldwide. This pathogen is associated with high morbidity and mortality rates. Moreover, *C. krusei* has shown intrinsic resistance to fluconazole, and the therapeutic use of this antifungal agent has been linked to numerous infections caused by this pathogen.[28]

Among the tested compounds (**3a–j**), compounds **3e** and **3f**, which carry a nitro substituent on phenyl ring, displayed a notable improvement in the spectrum of antifungal activity.

Anticancer activity

The synthesized compounds were screened *in vitro* against MDA-MB-231 and MCF-7 breast cancer cell lines to investigate potential cytotoxicity effects for 24 h (Table 2).

Compound **3e** with *N′*-(1-(4-nitrophenyl)methylidene)acetohydrazide moiety (nitro group at *para* position on phenyl ring) was found to be the most active derivative against breast MDA-MB-231 cell lines with IC_{50} value of 9.89 μM. Moreover, compounds **3b** and **3d** showed remarkable cytotoxicity against MDA-MB-231 cell lines. Compound **3f**, containing a 4-methoxy-3-nitrophenyl moiety, displayed the most potent antiproliferative activity with an IC_{50} value of 16.54 μM against

Table 1. The minimum inhibitory concentration (MIC) values of compounds **3a–j**.

MIC value (mg/ml)	Gram positive bacteria		Gram negative bacteria		Yeast		
Compound	*S. aureus*	*E. faecalis*	*P. aeruginosa*	*E. coli*	*C. albicans*	*C. parapsilosis*	*C. krusei*
3a	64	64	128	64	64	256	128
3b	256	128	256	64	64	128	64
3c	128	64	256	256	16	512	16
3d	256	128	256	256	64	64	32
3e	256	128	256	256	16	8	8
3f	128	64	256	256	16	32	32
3g	512	64	512	128	128	256	128
3h	512	256	512	256	128	256	128
3i	1024	128	512	256	256	128	128
3j	256	128	256	256	256	256	256
2	1024	512	256	256	256	256	256
Ciprofloxacin[a]	0.5	0.25	0.25	0.015	NA	NA	NA
Fluconazole[a]	NA[b]	NA	NA	NA	0.125	0.5	32

[a] Reference compounds, [b] Not applicable.

Table 2. Results of the CCK-8 assay presented as IC_{50} values obtained after 24 h of treatment.

Compound	IC_{50} (μM) MDA-MB-231	MCF-7
2	42.89 ± 1.29	53.47 ± 0.61
3a	63.67 ± 0.15	71.03 ± 0.43
3b	18.84 ± 2.84	30.53 ± 0.44
3c	23.12 ± 0.67	22.62 ± 0.67
3d	17.21±0.87	22.91±0.32
3e	9.89±1.02	39.55±0.71
3f	31.71±2.16	16.54±1.04
3g	45.11±1.76	31.54±0.62
3h	59.10±1.36	60.12±0.14
3i	39.51±0.41	17.52±0.15
3j	24.46±1.03	34.33±0.51
Cisplatin[a]	26.7 ± 1.70[29]	16.3 ± 2.30[29]

[a] Reference drug; IC_{50} refers to the half-maximal inhibitory concentration. The compounds were applied in three repetitions for the experimental and control groups (n = 3). Results are shown as mean ± SD.

the MCF-7 cell lines, followed by compound **3i** (4-fluoro-3-phenoxyphenyl substituent) showing potent cytotoxicity (IC_{50} = 17.52 μM).

The presence of a chlorine substitution on the phenyl moiety (**3g**) clearly led to a reduction in anticancer activity. This effect was further pronounced when two chlorine substituents were present, as observed in compound **3a**, resulting in a decreased anticancer activity against MDA-MB-231 cells. Also, the replacement of the 2-Cl group with 2-F or 2-OCF_3 groups led to an increase in cytotoxic activities. Intriguingly, the incorporation of bulkier substituents such as nitro and phenoxy at the 3rd position on the phenyl ring significantly enhanced the cytotoxicity against MCF-7 cells.

It was suggested that compound **3e**, which exhibited cytotoxicity based on the IC_{50} values, may have apoptotic potential. The apoptotic pathway can be divided into two pathways: intrinsic and extrinsic. Various caspases are involved in the intrinsic and extrinsic apoptotic pathways. The intrinsic pathway involves caspase-9 as the initiator caspase, while the extrinsic pathway involves caspase-8. Caspase-3/7 activation is observed in both pathways..[30] However, it has been previously shown that caspase-3 is not expressed in MCF-7 cells.[31] Considering this information, the effect of compound **3e** on the enzymatic activity of caspase-8, associated with the extrinsic apoptotic pathway, was investigated in MDA-MB-231 and MCF-7 cell lines. As shown in Figure 4, no significant changes in caspase-8 activity were observed ($p_{MDA\text{-}MB\text{-}231}$ = 0.521; $p_{MCF\text{-}7}$ = 0.368).

The intrinsic apoptotic pathway, also referred to as the mitochondrial pathway, involves the permeabilization of the outer mitochondrial membrane in response to a stimulus. This permeabilization leads to the release of cytochrome-c from the mitochondria into the cytosol, where it binds to Apaf-1 and triggers the activation of caspase-9. The permeabilization of the outer mitochondrial membrane is mostly associated with a loss of mitochondrial membrane potential.[32] To investigate the potential impact of compound **3e** on the intrinsic apoptotic pathway, changes in mitochondrial membrane potential were assessed using the JC-1 mitochondrial membrane potential assay.

While the fluorescence intensity appeared to rise with increasing concentrations of compound **3e** in both cell lines, no statistically significant changes were observed in the MCF-7 cell lines (Figure 5). Conversely, in the MDA-MB-231 cell lines, the fluorescence intensity in the 50 μM experimental group signifi-

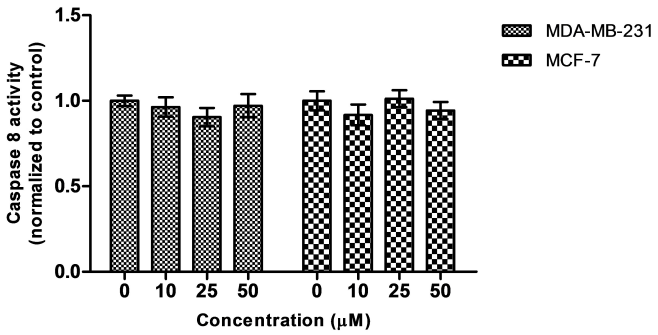

Figure 4. Effect of compound **3e** on the activity of caspase 8 in breast cancer cells.

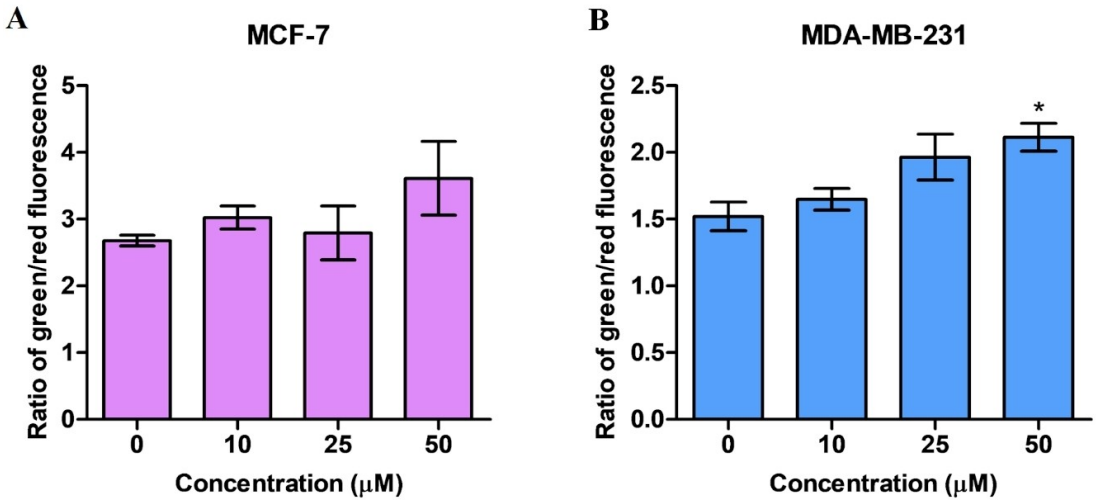

Figure 5. Green/red fluorescence intensity for JC-1 staining of MCF-7 (A) and MDA-MB-231 (B) cells after treatment of compound **3e** for 24h.

cantly increased compared to the control group, as depicted in Figure 5. Hence, it can be concluded that there was an increase in the permeability of the outer mitochondrial membrane and depolarization of the mitochondrial membrane potential.

The obtained results suggest that compound **3e** exhibits dose-dependent cytotoxicity, particularly in MDA-MB-231 triple-negative breast cancer cells. Furthermore, it appears to induce apoptosis through the mitochondrial pathway.

These findings provide further evidence that the nitro substituent on the phenyl ring of metacetamol hydrazide–hydrazone derivatives is responsible for their potent cytotoxicity and antifungal activity. Nitro groups are commonly found in approved drugs, particularly antibiotics, and are known to hinder the replication of microorganisms. The strong electron-withdrawing nature of the nitro moiety results in certain sections of the molecules becoming less polar, facilitating nonpolar interactions with essential proteins.[33] Additionally, the reduced nitro species can covalently bind to DNA, resulting in nuclear damage and subsequent cell death.[34]

Molecular docking studies

Molecules that interfere with the dynamics of microtubules/tubulin are extensively employed in cancer treatment. The majority of these compounds function through binding to tubulin protein which consists of α and β subunits and serves as the fundamental structure of microtubules.[35] The microtubule system serves as a crucial element in vital cellular processes like mitosis, intracellular movement, and maintaining cell morphology. Therefore, tubulin inhibition has emerged as a rational strategy for the development of potent anticancer agents.[36,37]

The colchicine site (represented in Figure 6) is one of the binding pockets found on tubulin that has significant potential for therapeutic applications. This particular site could potentially overcome some of the limitations associated with microtubule-targeting agents currently available in the market, such as taxanes and vinca alkaloids that target other sites of tubulin.[38]

Numerous structural scaffolds have been identified due to their potential to inhibit tubulin and thus display anticancer activity. Among them, hydrazone-based molecules, illustrated in Figure 7, are frequently reported as anti-tubulin agents that specifically target the colchicine binding site.[39–41]

Inspired by the structural similarity between our compounds and the hydrazones previously identified as colchicine binding site inhibitors of tubulin, we employed molecular modeling techniques to perform docking studies of compound **3e** within the corresponding binding pocket of tubulin (Figure 8).

We initially analyzed how the co-crystallized inhibitor Combretastatin A4 interacts with the colchicine binding site of tubulin and we determined the phenolic hydroxy group was responsible for forming hydrogen bond with Thr179. Additionally, Leu248, Ala250, Leu255, and Ala316 were significant residues participating in hydrophobic contacts with the inhibitor. Subsequently, we examined the most plausible docking pose of **3e** within the same binding pocket. Likewise the original inhibitor Combretastatin A4, **3e** formed a hydrogen bond with Thr179 through the N–H group of its acetamide moiety. Notably, an additional hydrogen bond was formed between the nitro group of **3e** and Tyr202. This situation highlights the importance of the substitution pattern of the phenyl ring. **3e** also engaged in lipophilic contacts with Leu248 and Ala250 through the phenyl ring of the metacetamol scaffold.

Based on the results obtained from molecular docking studies, it is plausible to suggest that compound **3e** demonstrates its antiproliferative effects by binding to the colchicine site of tubulin through comparable interactions as those of the original ligand Combretastatin A4.

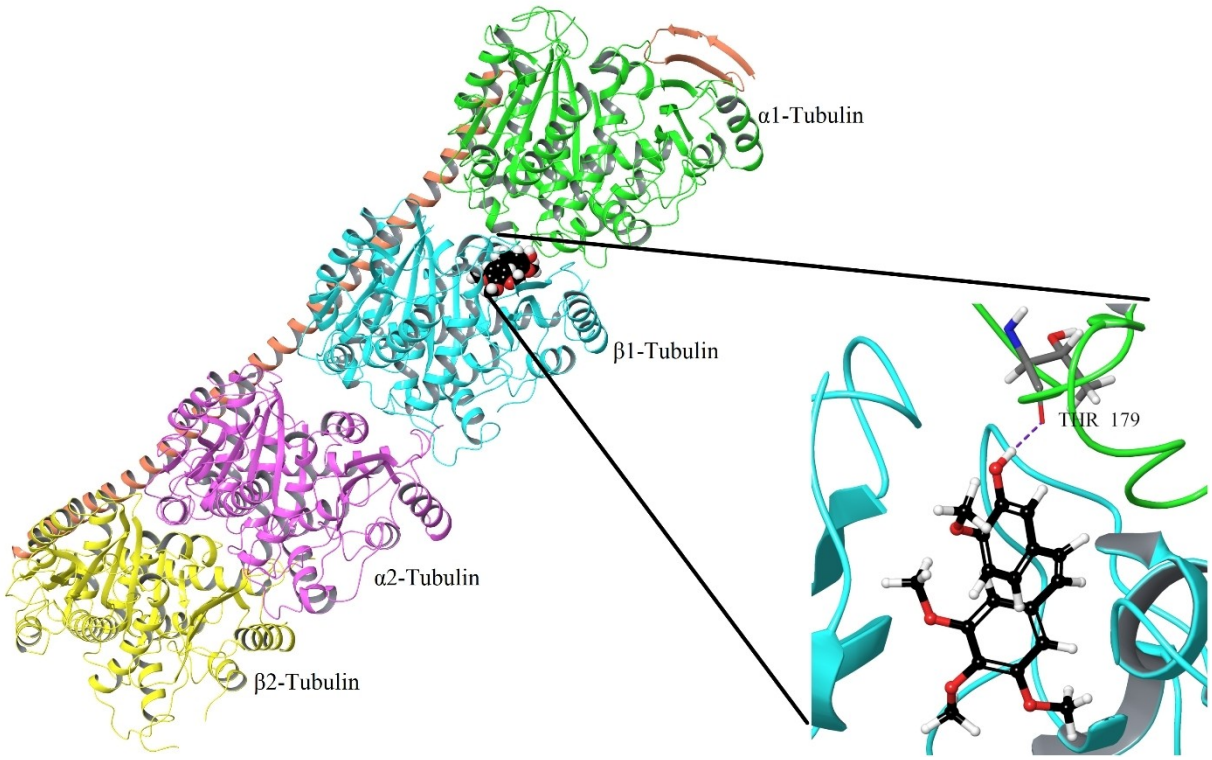

Figure 6. Two tubulin αβ heterodimers with combretastatin A4 bound to β subunit at the interface with α. Combretastatin A4 is shown as black ball&stick.

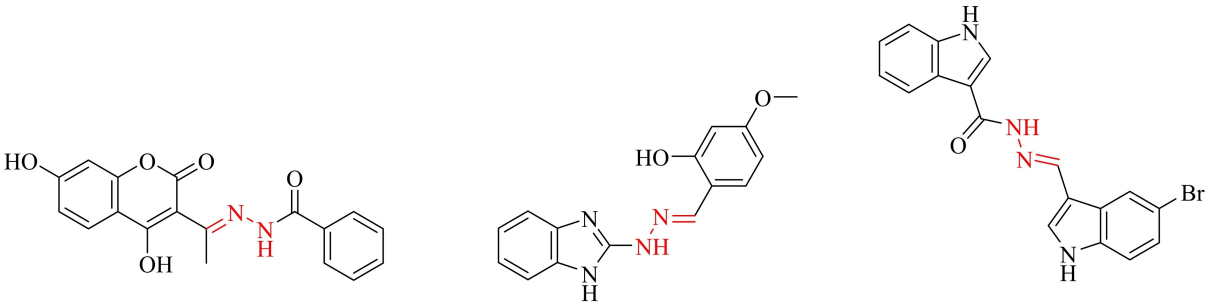

Figure 7. Recently reported hydrazone derivatives as anti-tubulin agents targeting colchicine binding site.

Conclusions

In summary, novel aryloxyacetic acid derivatives carrying hydrazone moiety were successfully synthesized starting from metacetamol by a convenient procedure. The antimicrobial and anticancer activities of the compounds were assessed against various microbial strains and breast cancer cell lines. Among them, *N*-(3-(2-(2-(4-nitrobenzylidene)hydrazinyl)-2-oxoethoxy)phenyl)acetamide (**3e**) exhibited the most potent antifungal properties against all *Candida* species, with MIC ranges of 8–16 μg/ml. Additionally, this compound (**3e**) showed promising anticancer activity against MDA-MB-231 breast cancer cells (IC_{50} = 9.89 μM). Mechanistic studies indicated that compound **3e** may inhibit cell proliferation by inducing a mitochondrial-dependent apoptotic pathway in MDA-MB-231 cells. Molecular docking studies suggested that **3e** is likely to represent its anticancer activity by targeting the colchicine binding site of tubulin. In conclusion, compound **3e** shows promise for further investigation in the development of new anticancer and antifungal agents.

Experimental Section

Chemistry

The chemicals and solvents used in this study were purchased from Merck and Sigma–Aldrich chemical companies and were exerted. All melting points (m.p.) of the compounds were determined in open capillaries using an Electrothermal Thermo Scientific IA9300 instrument and were uncorrected. The BRUKER Ultrashield TM spectrometer was used to record the NMR spectra. Microanalyses were determined using the LECO CHNS-932 instrument. The

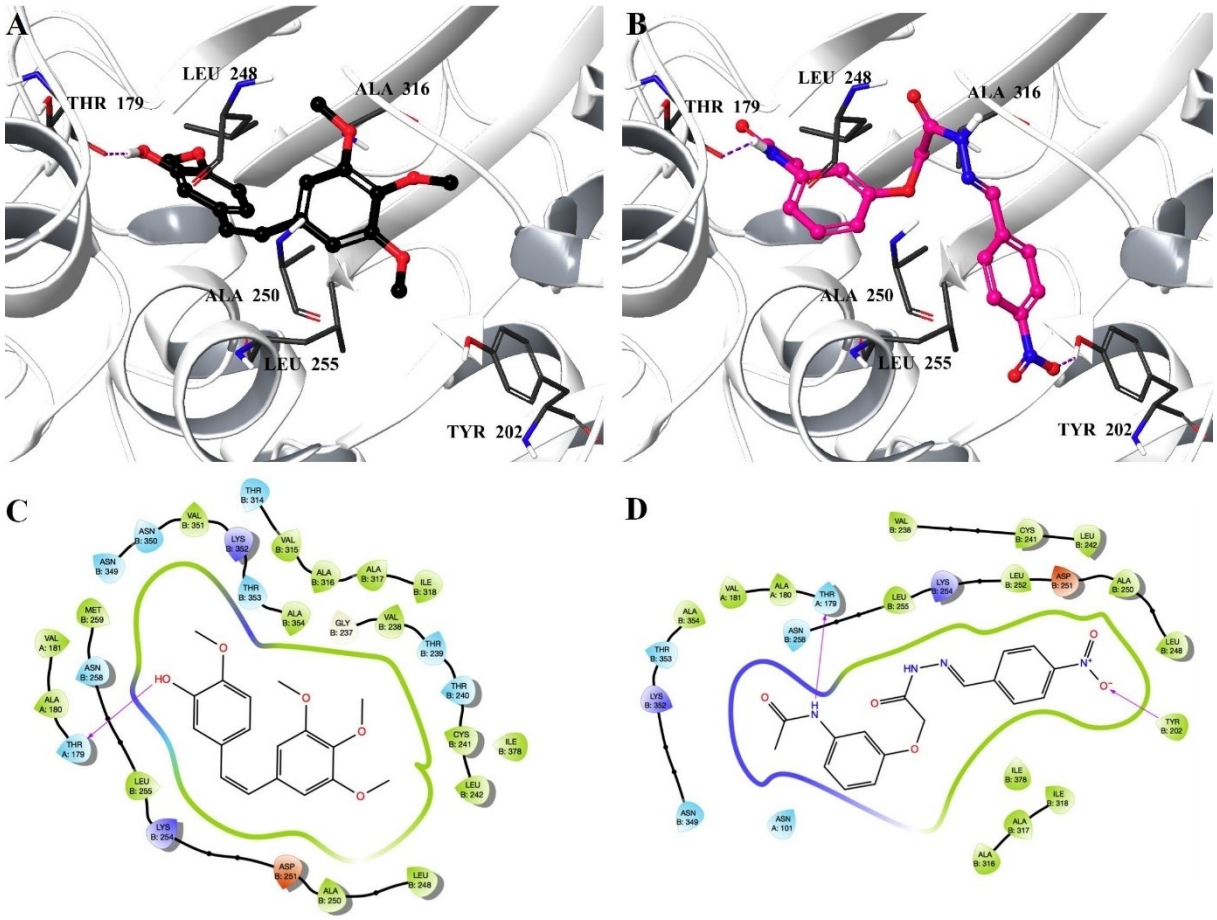

Figure 8. Binding mode of co-crystallized inhibitor Combretastatin A4 (A) and **3 e** (B) in the colchicine binding pocket of tubulin. 2D representations of ligand-protein interactions are also provided for Combretastatin A4 (C) and **3 e** (D). The ligands are depicted as sticks and balls in black (for Combretastatin A4) and pink (for **3 e**), while the amino acid residues interacting with them are shown as dark gray sticks. Protein backbone and hydrogen bonds are represented as white cartoon and purple dashes, respectively.

Shimazu 8400S spectrometer was used to record FT-IR spectra. The mass spectra were recorded on Shimadzu LC/MS/MS-8030 system. The synthesis of compounds **2** and **3** followed a previously reported procedure.[23,24] The spectra for each substances are provided as supplemental material.

General procedure for the synthesis of hydrazones (3 a–j)

A mixture of hydrazide **2** (1 mmol) and the appropriate aldehyde (1 mmol) in EtOH (20 mL) in the presence of a catalytic quantity of glacial acetic acid was refluxed for 3–4 h. After cooling the formed precipitate was filtered off and purified by crystallization using ethanol to give the hydrazone derivatives.

N-*(3-(2-(2-(2,5-Dichlorobenzylidene)hydrazinyl)-2-oxoethoxy)phenyl)acetamide (3 a)*

White solid; m.p. 229–231 °C; FT-IR υ_{max} (cm^{-1}): 3390 (N–H), 1705 (C=O), 1658 (C=O), 1608 (C=N); ^{1}H-NMR (300 MHz), (DMSO-d_6/TMS) δ ppm: 2.02 (s, 3H, $-COCH_3$), 4.66&5.17 (2s, 2H, $-OCH_2$), 6.59–8.01 (m, 7H, Ar–H), 8.33&8.69 (2s, 1H, CH=N), 9.91&9.97 (2s, 1H, NH), 11.89 (s, 1H, NH). ^{13}C-NMR (75 MHz), (DMSO-d_6/TMS) δ ppm: 24.5 (CH_3), 65.1&66.9 (CH_2), 105.8&106.2 (C-17), 109.3 (C-13), 111.9&112.5 (C-21), 126.3&126.6 (C-3), 129.7&129.9 (C-5), 131.9&132.0 (C-6), 132.7&132.9 (C-4), 133.4&133.6 (C-2), 138.9 (C-20), 140.8&140.9 (CH=N), 142.8 (C-18), 158.3&158.8 (C-16), 165.2 (C=O), 168.8,&169.8 (C=O). Anal. calc. for $C_{17}H_{15}Cl_2N_3O_3$,%: C, 53.70; H, 3.98; N, 11.05 Found, %: C, 53.78; H, 4.20; N, 11.17. LC/MS (ESI) *m/z*: 380.20 $[M+H]^+$, 378.25 $[M-H]^-$.

N-*(3-(2-(2-(4-((4-Fluorobenzyl)oxy)benzylidene)hydrazinyl)-2-oxoethoxy)phenyl)acetamide (3 b)*

White solid; m.p. 193–195 °C; FT-IR υ_{max} (cm^{-1}): 3358 (N–H), 1689 (C=O), 1658 (C=O), 1600 (C=N); ^{1}H-NMR (300 MHz), (DMSO-d_6/TMS) δ ppm: 2.02 (s, 3H, $-COCH_3$), 4.60&5.07 (2s, 2H, $-OCH_2$), 6.57-7.67 (m, 12H, Ar–H), 7.95&8.26 (2s, 1H, CH=N), 9.91&9.96 (2s, 1H, NH), 11.47&11.49 (2s, 1H, NH). ^{13}C-NMR (75 MHz), (DMSO-d_6/TMS) δ ppm: 24.4 (CH_3), 64.9,&66.8 (CH_2), 69.0 (OCH_2), 105.6&106.1 (C-2), 109.3 (C-4), 111.8&112.4 (C-6), 115.5,&115.8 (C-28, C-30), 127.2&127.3 (C-19, C-21), 128.9&129.1 (C-17), 129.7&129.8 (C-18, C-22), 130.4&130.5 (C-27, C-31), 133.3 (C-26), 133.4 (C-5), 140.8&140.9 (CH=N), 143.9 (C-3), 148.0 (C-20), 158.4&158.8 (C-1), 162.2 (C–F, d, $J=242$), 164.3 (C=O), 168.7&169.1 (C=O). Anal. calc. for $C_{24}H_{22}FN_3O_4$,%: C, 66.20; H, 5.09; N, 9.65 Found, %: C, 66.15; H, 5.36; N, 9.66. LC/MS (ESI) *m/z*: 436.35 $[M+H]^+$, 434.35 $[M-H]^-$.

N-*(3-(2-Oxo-2-(2-(2-(trifluoromethoxy)benzylidene)hydrazinyl)ethoxy)phenyl)acetamide (3 c)*

Beige solid; m.p. 189–191 °C; FT-IR υ_{max} (cm^{-1}): 3254 (N–H), 1681 (C=O), 1660 (C=O), 1602 (C=N); ^{1}H-NMR (300 MHz), (DMSO-d_6/TMS) δ ppm: 2.02 (s, 3H, –$COCH_3$), 4.64&5.12 (2s, 2H, –OCH_2), 6.59–8.08 (m, 8H, Ar–H), 8.28&8.63 (2s, 1H, CH=N), 9.91&9.97 (2s, 1H, NH), 11.71&11.87 (2s, 1H, NH). ^{13}C-NMR (75 MHz), (DMSO-d_6/TMS) δ ppm: 24.5 (CH_3), 65.0&66.9 (CH_2), 105.7&106.2 (C-20), 109.3 (C-22), 111.9&112.5 (C-24), 118.8 (C-6), 122.2 (OCF_3, q, J = 256), 127.0&127.3 (C-3), 127.4&127.6 (C-4), 129.8&129.9 (C-2), 132.0&132.2 (C-5), 137.6 (C-23), 140.9 (CH=N), 141.4 (C-21), 147.0 (C-1), 158.4&158.8 (C-19), 165.0 (C=O), 168.7&169.5 (C=O). Anal. calc. for $C_{18}H_{16}F_3N_3O_4$.3/4 H_2O,%: C, 52.88; H, 4.31; N,10.28 Found, %: C, 52.66; H, 4.35; N, 10.80. LC/MS (ESI) *m/z*: 396.25 $[M+H]^+$, 394.30 $[M-H]^-$.

N-*(3-(2-(2-(2-Fluorobenzylidene)hydrazinyl)-2-oxoethoxy)phenyl)acetamide (3 d)*

Off-white solid; m.p. 192–194 °C; FT-IR υ_{max} (cm^{-1}): 3304 (N–H), 1697 (C=O), 1666 (C=O), 1604 (C=N); ^{1}H-NMR (300 MHz), (DMSO-d_6/TMS) δ ppm: 2.02 (s, 3H, –$COCH_3$), 4.63&5.11 (2s, 2H, –OCH_2), 6.58-7.94 (m, 8H, Ar–H), 8.22&8.59 (2s, 1H, CH=N), 9.92&9.97 (2s, 1H, NH), 11.72&11.75 (2s, 1H, NH). ^{13}C-NMR (75 MHz), (DMSO-d_6/TMS) δ ppm: 24.5 (CH_3), 65.0&66.9 (CH_2), 105.7&106.2 (C-2), 109.3 (C-4), 111.9&112.5 (C-6), 116.3&116.6 (C-19), 121.9&122.0 (C-21), 126.9 (C-17), 129.9 (C-22), 132.3 (C-20), 137.1 (C-5), 140.9 (CH=N), 141.1 (C-3), 158.4&158.8 (C-1), 161.1 (C–F,d, J = 247), 164.8 (C=O), 168.8&169.5 (C=O). Anal. calc. for $C_{17}H_{16}FN_3O_3$.1/2 H_2O,%: C, 60.35; H, 5.06; N, 12.42 Found, %: C, 62.00; H, 4.90; N, 12.76. LC/MS (ESI) *m/z*: 331.30 $[M+2H]^+$, 328.30 $[M-H]^-$.

N-*(3-(2-(2-(4-Nitrobenzylidene)hydrazinyl)-2-oxoethoxy)phenyl)acetamide (3 e)*

Off-white solid; m.p. 241–242 °C; FT-IR υ_{max} (cm^{-1}): 3346 (N–H), 1697 (C=O), 1649 (C=O), 1606 (C=N); ^{1}H-NMR (300 MHz), (DMSO-d_6/TMS) δ ppm: 2.02 (s, 3H, –$COCH_3$), 4.67&5.15 (2s, 2H, –OCH_2), 6.64–8.44 (m, 9H, Ar–H &CH=N), 9.92&9.97 (2s, 1H, NH), 11.92 (s, 1H, NH). ^{13}C-NMR (75 MHz), (DMSO-d_6/TMS) δ ppm: 24.5 (CH_3), 65.1, 66.8 (CH_2), 105.8&106.2 (C-2), 109.3 (C-4), 112.0 (C-6), 124.4&124.5 (C-19, C-21), 128.3&128.5 (C-18, C-22), 129.8&129.9 (C-17), 140.9&140.9 (CH=N), 141.9 (C-5), 145.8 (C-3), 148.3 (C-20), 158.4&158.8 (C-1), 165.2 (C=O), 168.9&169.8 (C=O). Anal. calc. for $C_{17}H_{16}FN_4O_5$,%: C, 57.3; H, 4.53; N, 15.72 Found, %: C, 57.25; H, 4.35; N, 15.79. LC/MS (ESI) *m/z*: 357.30 $[M+H]^+$, 355.35 $[M-H]^-$.

N-*(3-(2-(2-(4-Methoxy-3-nitrobenzylidene)hydrazinyl)-2-oxoethoxy)phenyl)acetamide (3 f)*

Yellow solid; m.p. 252–254 °C; FT-IR υ_{max} (cm^{-1}): 3375 (N–H), 1687 (C=O), 1656 (C=O), 1599 (C=N); ^{1}H-NMR (300 MHz), (DMSO-d_6/TMS) δ ppm: 2.02 (s, 3H, –$COCH_3$), 3.97 (s, 3H, –OCH_3), 4.63&5.12 (2s, 2H, –OCH_2), 6.63–8.32 (m, 8H, Ar–H &CH=N), 9.91&9.96 (2s, 1H, NH), 11.69 (s, 1H, NH). ^{13}C-NMR (75 MHz), (DMSO-d_6/TMS) δ ppm: 24.5 (CH_3), 57.4 (OCH_3), 65.1&66.8 (CH_2), 105.8&106.2 (C-20), 109.3 (C-22), 111.9&112.4 (C-24), 115.0&115.2 (C-6), 123.3&123.8 (C-3), 127.2 (C-4), 129.7&129.9 (C-5), 132.8 (C-23), 140.1&140.8 (C-2), 140.9&141.9 (CH=N), 145.9 (C-21), 153.1&153.5 (C-1), 158.4&158.8 (C-19), 164.7 (C=O), 168.8&169.5 (C=O). Anal. calc. for $C_{18}H_{18}N_4O_6$,%: C, 55.96; H, 4.70; N, 14.50 Found, %: C, 55.60; H, 4.51; N, 14.48. LC/MS (ESI) *m/z*: 387.30 $[M+H]^+$, 385.25 $[M-H]^-$.

N-*(3-(2-(2-(2-Chlorobenzylidene)hydrazinyl)-2-oxoethoxy)phenyl)acetamide (3 g)*

Off-white solid; m.p. 201–203 °C; FT-IR υ_{max} (cm^{-1}): 3336 (N–H), 1697 (C=O), 1660 (C=O), 1599 (C=N); ^{1}H-NMR (300 MHz), (DMSO-d_6/TMS) δ ppm: 2.02 (s, 3H, –$COCH_3$), 4.59&5.03 (2s, 2H, –OCH_2), 6.53-7.59 (m, 8H, Ar–H), 7.97&8.28 (2s, 1H, CH=N), 9.91&9.92 (2s, 1H, NH), 11.63&11.65 (s, 1H, NH). ^{13}C-NMR (75 MHz), (DMSO-d_6/TMS) δ ppm: 24.5 (CH_3), 65.1&66.9 (CH_2), 105.7&106.2 (C-16), 109.4 (C-18), 111.9&112.5 (C-20), 127.&127.4 (C-3), 128.0 (C-4), 129.8&129.9 (C-5), 130.3 (C-6), 131.6&131.8 (C-2), 132.0 (C-1), 133.4 (C-19), 140.2&140.9 (CH=N), 144.2 (C-17), 158.4&158.8 (C-15), 164.9 (C=O), 168.7&169.5 (C=O). Anal. calc. for $C_{17}H_{16}ClN_3O_3$. 1/4 H_2O,%: C, 58.29; H, 4.75; N, 12.00 Found, %: C, 58.63; H, 4.61; N, 12.01. LC/MS (ESI) *m/z*: 346.25 $[M+H]^+$, 344.30 $[M-H]^-$.

N-*(3-(2-(2-(3,4-Difluorobenzylidene)hydrazinyl)-2-oxoethoxy)phenyl)acetamide (3 h)*

Beige solid; m.p. 202–204 °C; FT-IR υ_{max} (cm^{-1}): 3342 (N–H), 1693 (C=O), 1651 (C=O), 1608 (C=N); ^{1}H-NMR (300 MHz), (DMSO-d_6/TMS) δ ppm: 2.02 (s, 3H, –$COCH_3$), 4.63&5.12 (2s, 2H, –OCH_2), 6.59-7.87 (m, 7H, Ar–H), 7.98&8.31 (2s, 1H, CH=N), 9.91&9.96 (2s, 1H, NH), 11.71&11.73 (s, 1H, NH). ^{13}C-NMR (75 MHz), (DMSO-d_6/TMS) δ ppm: 24.5 (CH_3), 65.1& 66.8 (CH_2), 105.8&106.2 (C-2), 109.2 (C-4), 111.9&112.4 (C-6), 115.5&115.7 (C-21), 118.3&118.5 (C-18), 124.8 (C-22), 129.8&129.9 (C-17), 132.3 (C-5), 140.8&140.9 (CH=N), 141.9 (C-3), 158.4&158.8 (C-1), 160.7 (C–F, d, J = 248), 161.1 (C–F, d, J = 254), 164.8 (C=O), 168.7&169.6 (C=O). Anal. calc. for $C_{17}H_{15}F_2N_3O_3$,%: C, 58.79; H, 4.35; N, 12.10 Found, %: C, 58.50; H, 4.14; N, 11.77. LC/MS (ESI) *m/z*: 348.25 $[M+H]^+$, 346.35 $[M-H]^-$.

N-*(3-(2-(2-(4-Fluoro-3-phenoxybenzylidene)hydrazinyl)-2-oxoethoxy)phenyl)acetamide (3 i)*

White solid; m.p. 163–165 °C; FT-IR υ_{max} (cm^{-1}): 3281 (N–H), 1697 (C=O), 1674 (C=O), 1585 (C=N); ^{1}H-NMR (300 MHz), (DMSO-d_6/TMS) δ ppm: 2.02 (s, 3H, –$COCH_3$), 4.59&5.03 (2s, 2H, –OCH_2), 6.53-7.58 (m, 12H, Ar–H), 7.97&8.28 (2s, 1H, CH=N), 9.91&9.96 (2s, 1H, NH), 11.64 (s, 1H, NH). ^{13}C-NMR (75 MHz), (DMSO-d6/TMS) δ ppm: ^{13}C-NMR (75 MHz), (DMSO-d_6/TMS) δ ppm: 24.5 (CH_3), 65.0&66.8 (CH_2), 105.8&106.2 (C-23), 109.2 (C-25), 111.9&112.4 (C-22), 117.3&117.9 (C-6), 118.0&118.4 (C-3), 120.4 (C-11), 123.9&124.2 (C-4), 129.8&129.9 (C-9, C-13), 130.5&130.6 (C-10, C-12), 132.2 (C-26), 134.1 (C-5), 140.8&140.9 (CH=N), 142.5 (C-24), 156.3&156.6 (C-1), 156.8&157.1 (C-8), 158.4&158.8 (C-22), 164.7 (C=O), 168.8&169.6 (C=O). Anal. calc. for $C_{23}H_{20}FN_3O_4$,%: C, 65.55; H, 4.78; N, 9.97 Found, %: C, 65.23; H, 5.26; N, 10.14. LC/MS (ESI) *m/z*: 422.35 $[M+H]^+$, 420.35 $[M-H]^-$.

N-*(3-(2-Oxo-2-(2-(4-(trifluoromethoxy)benzylidene)hydrazinyl)ethoxy)phenyl)acetamide (3 j)*

Off-white solid; m.p. 186–188 °C; FT-IR υ_{max} (cm^{-1}): 3296 (N–H), 1697 (C=O), 1654 (C=O), 1600 (C=N); ^{1}H-NMR (300 MHz), (DMSO-d_6/TMS) δ ppm: 2.02 (s, 3H, –$COCH_3$), 4.64&5.11 (2s, 2H, –OCH_2), 6.59-7.87 (m, 8H, Ar–H), 8.04–8.36 (2s, 1H, CH=N), 9.92&9.97 (2s, 1H, NH), 11.71 (s, 1H, NH). ^{13}C-NMR (75 MHz), (DMSO-d_6/TMS) δ ppm: 24.2 (CH_3), 64.7&66.5 (CH_2), 105.4&105.9 (C-2), 109.0 (C-4), 111.6&112.2 (C-6), 121.7 (OCF_3, q, J = 248), 128.9&129,1 (C-19, C-21), 129.5&129.6 (C-18, C-22), 133.4 (C-17), 133.6 (C-5), 140.6&140.7 (CH=N), 142.3 (C-3), 146.4 (C-20), 158.1&158.5 (C-1), 164.5 (C=O), 168.5&169.2 (C=O). Anal. calc. for $C_{18}H_{16}F_3N_3O_4.H_2O$,%: C, 52.30; H, 4.39; N,10.17 Found,

%: C, 52.08; H, 4.53 N, 10.34. LC/MS (ESI) *m/z*: 397.30 $[M+2H]^+$, 394.30 $[M-H]^-$.

Biological Assays

Antimicrobial activity testing by broth microdilution

In vitro antimicrobial activity assays were carried out by broth microdilution method according to the Clinical and Laboratory Standards Institute (CLSI) guidelines against a panel of reference bacterial strains including *S. aureus* ATCC 29213, *E. faecalis* ATCC 29212, *E. coli* ATCC 25922, *P. aeruginosa* ATCC 27853 and yeast strains including *C. albicans* ATCC 90028, *C. parapsilosis* ATCC 90018, *C. krusei* ATCC 6258.[42,43]

The stock solutions of the test compounds were dissolved in dimethyl sulfoxide (DMSO) and twofold serial dilutions were prepared in 96-well polystyrene plates containing either Mueller–Hinton Broth (MHB, Merck, Germany) for bacteria or RPMI 1640 buffered to a pH of 7 with MOPS for yeasts in a concentration range of 1024 μg/ml to 0.5 μg/mL. Ciprofloxacin and fluconazole were used as control drugs for tested bacteria and fungi, respectively.

Microbial suspensions were prepared from fresh overnight cultures of each microorganism and adjusted to 0.5 McFarland standard. The suspensions were subsequently diluted in MHB or RPMI 1640 and added to each well to give a final cell density of 2.5×10^3 cfu/mL for yeasts and 5×10^5 cfu/mL for bacteria. Sterility control and growth control were included in each assay. MICs were read after incubation at 37 °C for 24 h.

Anticancer activity assay

Cell culture

MDA-MB-231 triple negative and MCF-7 luminal A breast cancer cell lines were incubated in DMEM medium containing 10% FBS and 1% Penicillin/Streptomycin at 37 °C and 5% CO_2. The medium was changed three times a week.

Cell viability and cytotoxicity

CCK-8 colorimetric method was used to determine the effect of metacetamol and its derivatives on cell viability and cytotoxicity in vitro. In this method, cells were seeded at 5000 cells/well in 96-well plates. After 24 h, control and experimental groups were formed with three repetitions in each group. Compounds for the experimental group were diluted at appropriate concentrations (10, 25, 50, 75, 100 μM). After 24 h of incubation, the medium in the wells was discarded. 100 μl of fresh medium and 10 μl of WST-8 solution were added to each well (Cell Counting Kit-8, KTC011001, Abbkine). After 4 h, the absorbance value was measured at 450 nm wavelength (Synergy H1, BioTek Instruments Inc., USA).

Caspase-8 enzymatic activity

50 000 cells/well were seeded in 96-well black opaque plates. After overnight incubation, control (0 μM) and experimental (10, 25, 50 μM) groups were formed for the metacetamol derivative (**3 e**), with three replicates in each group. After 24 h, the medium in the wells was discarded. A working solution for Caspase-8 was prepared as specified in the manufacturer's protocol. Then, 100 μl of the working solution was added to each well. After 1 h at room temperature, fluorescence values were measured at 490 and 525 nm excitation and emission wavelengths (Cell Meter Caspase 3/7,8,9 Activity Apoptosis assay kit, 22820, AAT Bioquest, Sunnyvale, USA).

JC-1mitochondrial membrane potential test

50 000 cells/well were seeded in 96-well black opaque plates. After overnight incubation, control (0 μM) and experimental (10, 25, 50 μM) groups were formed for the metacetamol derivative (**3 e**), with three replicates in each group. After 24 h, the medium in the wells was discarded. Then, 100 μl of fresh medium and 1 : 10 diluted JC-1 dye were added to each well (JC-1 Mitochondrial Membrane Potential Assay Kit, 10009172, Cayman Chemical). Centrifugation and buffering were performed as specified in the manufacturer's protocol. Fluorescence values were measured with Elisa Reader, with excitation and emission wavelengths being 535 and 595 nm for healthy cells, and 485 and 535 nm for apoptotic cells, respectively.

Statistical analysis

GraphPad Prism (version 5.01, GraphPad Software, CA, USA) program was used for statistical analysis of the obtained data. Dunn's multiple comparison test was applied after one-way ANOVA test. The significance value was accepted for $p<0.05$.

Molecular Docking

The 3D crystal structure of the tubulin-combretastatin A4 complex was downloaded from the Protein Data Bank with PDB code 5LYJ.[44] The chemical structure of compound **3 e** was drawn, energy minimized and docked into the colchicine binding site of tubulin using LigandScout 4.4[45] and AutoDock 4.2 with default parameters.[46] The resulting docking poses were visually analyzed and the docking figures were prepared using Maestro.[47]

Author Contributions

S. Ş. and S. G. K. contributed to conception and design of the study. S. Ş. and E. Ç. conducted the research. E. Ç. and I. A. collected data. I. A., P. M. T., O. O., Ş. N. and C. Ö. analyzed and interpreted the results. M. G. G. performed the molecular docking studies. S. Ş., I. A., P. M. T., O. O. and M. G. G. contributed to manuscript preparation. All authors reviewed the results and approved the final version of the manuscript.

Acknowledgements

The authors would like to thank TUBITAK [2209-A] for partially providing financial support (Project No: 1919B012202388). M. G. G. would like to thank Prof. Dr. Gerhard Wolber, Freie Universität Berlin, for providing the license for LigandScout 4.4.

Conflict of Interests

The authors declare no conflict of interest.

Data Availability Statement

The data that support the findings of this study are available in the supplementary material of this article.

Keywords: Antimicrobial · cancer · hydrazones · metacetamol · molecular docking

[1] D. K. Biswas, L. Averboukh, S. Sheng, K. Martin, D. S. Ewaniuk, T. F. Jawde, F. Wang, A. B. Pardee, *Mol. Med.* **1998**, *4*, 454–467.
[2] N. Roodi, L. R. Bailey, W.-Y. Kao, C. S. Verrier, C. J. Yee, W. D. Dupont, F. F. Parl, *J. Natl. Cancer Inst.* **1995**, *87*, 446–451.
[3] K. K. Kumarasamy, M. A. Toleman, T. R. Walsh, J. Bagaria, F. Butt, R. Balakrishnan, U. Chaudhary, M. Doumith, C. G. Giske, S. Irfan, P. Krishnan, A. V. Kumar, S. Maharjan, S. Mushtaq, T. Noorie, D. L. Paterson, A. Pearson, C. Perry, R. Pike, B. Rao, U. Ray, J. B. Sarma, M. Sharma, E. Sheridan, M. A. Thirunarayan, J. Turton, S. Upadhyay, M. Warner, W. Welfare, D. M. Livermore, N. Woodford, *Lancet Infect. Dis.* **2010**, *10*, 597–602.
[4] J. Guinea, *Clin. Microbiol. Infect.* **2014**, *20*, 5–10.
[5] C.-Y. Low, C. Rotstein, *Med Rep.* **2011**, *3*, 14.
[6] G. Bashir Sher-i-Kashmir, J. Ahmad, G. M. C. Baramulla, *Int. J. Adv. Res.* **2014**, *2*, 541–550.
[7] S. Rollas, Ş. G. Küçükgüzel, *Molecules* **2007**, *12*, 1910–1939.
[8] S. Şenkardeş, D. Kart, B. Bebek, M. G. Gündüz, Ş. G. Küçükgüzel, *J. Biomol. Struct. Dyn.* **2022**, *0*, 1–12.
[9] E. M. Mohi El-Deen, E. S. Nossier, E. A. Karam, *Sci. Pharm.* **2022**, *90*, 52.
[10] S. Mistry, A. K. Singh, *Future J. Pharm. Sci.* **2022**, *8*.
[11] A. N. Yankin, N. V. Nosova, V. V. Novikova, V. L. Gein, *Russ. J. Gen. Chem.* **2022**, *92*, 166–173.
[12] S. Şenkardeş, M. E. Kiymaci, K. Kale, İ. M. Kozanoğlu, B. Kaşkatepe, G. Küçükgüzel, *J. Res. Pharm.* **2021**, *25*, 135–141.
[13] S. Şenkardeş, M. İhsan Han, M. Gürboğa, Ö. B. Özakpinar, Güniz Küçükgüzel, *Med. Chem. Res.* **2022**, *31*, 368–379.
[14] M. İ. Han, P. Atalay, C. Ü. Tunç, G. Ünal, S. Dayan, Ö. Aydın, G. Küçükgüzel, *Bioorg. Med. Chem.* **2021**, *37*, 116097.
[15] H. C. Koç, İ. Atlihan, P. Mega-Tiber, O. Orun, G. Küçükgüzel, *J. Res. Pharm.* **2022**, *26*, 1–12.
[16] M. İ. Han, Ö. D. Yeşil Baysal, G. Ş. Başaran, G. Sezer, D. Telci, Ş. G. Küçükgüzel, *Tetrahedron* **2022**, *115*, 132797.
[17] S. M. Gomha, Z. A. Muhammad, H. M. Abdel-aziz, I. K. Matar, A. A. El-Sayed, *Green Chem. Lett. Rev.* **2020**, *13*, 6–17.
[18] M. S. Ibrahim, B. Farag, J. Y. Al-Humaidi, M. E. A. Zaki, M. Fathalla, S. M. Gomha, *Molecules* **2023**, *28*, 3869.
[19] A. R. Sayed, S. M. Gomha, H. M. Abd El-lateef, T. Z. Abolibda, *Green Chem. Lett. Rev.* **2021**, *14*, 180–189.
[20] P. N. Bandeira, T. L. G. Lemos, H. S. Santos, M. C. S. de Carvalho, D. P. Pinheiro, M. O. de Moraes Filho, C. Pessoa, F. W. A. Barros-Nepomuceno, T. H. S. Rodrigues, P. R. V. Ribeiro, H. S. Magalhães, A. M. R. Teixeira, *Med. Chem. Res.* **2019**, *28*, 2037–2049.
[21] N. Kulabaş, E. Tatar, Ö. Bingöl Özakpınar, D. Özsavcı, C. Pannecouque, E. De Clercq, İ. Küçükgüzel, *Eur. J. Med. Chem.* **2016**, *121*, 58–70.
[22] L. Chen, P. Wang, Z. Li, L. Zhou, Z. Wu, B. Song, S. Yang, *Chin. J. Chem.* **2016**, *34*, 1236–1244.
[23] S. Wang, H. Liu, K. Lei, G. Li, J. Li, Y. Wei, X. Wang, R. Liu, *Bioorg. Chem.* **2020**, *103*, 104182.
[24] B. Nimavat, S. Mohan, J. Saravanan, M. P. Patel, S. Deka, A. Talukdar, M. Basak, R. K. Sarma, *Asian J. Chem.* **2013**, *25*, 1691–1694.
[25] R. Munir, N. Javid, M. Zia-ur-Rehman, M. Zaheer, R. Huma, A. Roohi, M. M. Athar, *Molecules* **2021**, *26*, 4908.
[26] S. Şenkardeş, A. Türe, S. Ekrek, A. T. Durak, M. Abbak, Ö. Çevik, B. Kaşkatepe, İ. Küçükgüzel, Güniz Küçükgüzel, *J. Mol. Struct.* **2021**, *1223*, 1–9.
[27] A. B. Lopes, E. Miguez, A. E. Kümmerle, V. M. Rumjanek, C. A. M. Fraga, E. J. Barreiro, *Molecules* **2013**, *18*, 11683–11704.
[28] K. Gill, S. Kumar, I. Xess, S. Dey, *Indian J. Med. Microbiol.* **2015**, *33*, 110–116.
[29] M. Stompor, M. Świtalska, J. Wietrzyk, *Acta Biochim. Pol.* **2019**, *66*, 559–565.
[30] C. Y. Looi, A. Arya, F. K. Cheah, B. Muharram, K. H. Leong, K. Mohamad, W. F. Wong, N. Rai, M. R. Mustafa, *PLoS One* **2013**, *8*, e56643.
[31] R. U. Jänicke, *Breast Cancer Res. Treat.* **2009**, *117*, 219–221.
[32] J. E. Chipuk, L. Bouchier-Hayes, D. R. Green, *Cell Death Differ.* **2006**, *13*, 1396–1402.
[33] S. Noriega, J. Cardoso-Ortiz, A. López-Luna, M. D. R. Cuevas-Flores, J. A. Flores De La Torre, *Pharmaceuticals* **2022**, *15*, 717.
[34] J. Müller, A. Hemphill, N. Müller, *Int. J. Parasitol. Drugs Drug Resist.* **2018**, *8*, 271–277.
[35] A. Roll-Mecak, *Dev. Cell* **2020**, *54*, 7–20.
[36] R. Kaur, G. Kaur, R. K. Gill, R. Soni, J. Bariwal, *Eur. J. Med. Chem.* **2014**, *87*, 89–124.
[37] K. Haider, S. Rahaman, M. S. Yar, A. Kamal, *Expert Opin. Ther. Pat.* **2019**, *29*, 623–641.
[38] Y. Ren, Y. Wang, G. Li, Z. Zhang, L. Ma, B. Cheng, J. Chen, *J. Med. Chem.* **2021**, *64*, 4498–4515.
[39] P. Govindaiah, N. Dumala, I. Mattan, P. Grover, M. Jaya Prakash, *Bioorg. Chem.* **2019**, *91*, 103143.
[40] M. Argirova, M. Guncheva, G. Momekov, E. Cherneva, R. Mihaylova, M. Rangelov, N. Todorova, P. Denev, K. Anichina, A. Mavrova, D. Yancheva, *Molecules* **2023**, *28*, 291.
[41] D. Das Mukherjee, N. M. Kumar, M. P. Tantak, S. Datta, D. Ghosh Dastidar, D. Kumar, G. Chakrabarti, *Biochim. Biophys. Acta Mol. Cell Res.* **2020**, *1867*, 118762.
[42] *Clinical and Laboratory Standards Institute, Methods for Dilution Antimicrobial Susceptibility Tests for Bacteria That Grow Aerobically, Approved Standard 11th Ed., M 07-A8. Clinical and Laboratory Standards Institute, Wayne, PA*, **2018**.
[43] *Clinical and Laboratory Standards Institute, Reference Method for Broth Dilution Antifungal Susceptibility Testing of Yeasts: Approved Standard 4th Ed., M 27-A4. Clinical and Laboratory Standards Institute, Wayne, PA*, **2017**.
[44] R. Gaspari, A. E. Prota, K. Bargsten, A. Cavalli, M. O. Steinmetz, *Chem* **2017**, *2*, 102–113.
[45] G. Wolber, T. Langer, *J. Chem. Inf. Model.* **2005**, *45*, 160–169.
[46] G. M. Morris, R. Huey, W. Lindstrom, M. F. Sanner, R. K. Belew, D. S. Goodsell, A. J. Olson, *J. Comput. Chem.* **2009**, *30*, 2785–2791.
[47] Schrödinger Release 2019–1: Maestro, Schrödinger, LLC, New York, NY. **2019**.

Manuscript received: May 25, 2023
Accepted manuscript online: July 7, 2023
Version of record online: ■■, ■■■